2,2'-Bipyrimidine (bipym)-bridged Dinuclear Complexes. Part 2.[1] Synthesis, Crystal Structure and Magnetic Properties of $[Fe_2(H_2O)_8(bipym)][SO_4]_2\cdot 2H_2O$ and $[Fe_2(H_2O)_6(bipym)(SO_4)_2]$†

Enrique Andrés,[a] Giovanni De Munno,[b] Miguel Julve,*[,a] José Antonio Real[a] and Francesc Lloret[a]

[a] *Departament de Química Inorgànica, Facultat de Química de la Universitat de València, Dr. Moliner 50, 46100 Burjassot (València), Spain*

[b] *Dipartimento di Chimica, Università degli Studi della Calabria, 87030 Arcavacata di Rende (Cosenza), Italy*

Two new dinuclear iron(II) complexes of formulae $[Fe_2(H_2O)_8(bipym)][SO_4]_2\cdot 2H_2O$ **1** and $[Fe_2(H_2O)_6(bipym)(SO_4)_2]$ **2** (bipym = 2,2'-bipyrimidine) have been synthesised and their crystal structures determined by single-crystal X-ray diffraction. Crystals of **1** and **2** are monoclinic, space group $P2_1/c$ with $a = 8.138(1)$, $b = 11.661(2)$, $c = 11.886(2)$ Å, $\beta = 91.85(1)°$ and $Z = 2$ for **1** and space group $P2_1/n$ with $a = 6.275(2)$, $b = 13.550(4)$, $c = 10.937(2)$ Å, $\beta = 96.43(2)°$ and $Z = 2$ for **2**. The structure of **1** consists of centrosymmetric dinuclear cations $[Fe_2(H_2O)_8(bipym)]^{4+}$, unco-ordinated sulfate anions and water of crystallization whereas that of **2** is made up of neutral dinuclear $[Fe_2(H_2O)_6(bipym)(SO_4)_2]$ units. The co-ordination geometry around each iron atom is that of a highly distorted octahedron: the Fe^{II}–N distances are longer (average value 2.22 Å) than the Fe^{II}–O ones (average values 2.11 and 2.09 in **1** and **2**, respectively). In both complexes, the bipyrimidine group joins two adjacent iron atoms acting in a bis(chelating) fashion. The C–C bond between the pyrimidine rings of bipym is perpendicular to the Fe ··· Fe vector giving two five-membered chelate rings, the bite angle of bipym being 74.9(1)° in **1** and 74.1(1)° in **2**. The intramolecular metal–metal separation is 5.836(1) and 5.909(1) Å in **1** and **2**, respectively. Magnetic susceptibility *versus* temperature data for both compounds were fitted to the Heisenberg–Dirac–Van-Vleck $S_1 = S_2 = 2$ spin exchange model with $J = -3.4$ cm^{-1}, $g = 2.28$ and $\theta = -0.7$ cm^{-1} for **1** and $J = -3.1$ cm^{-1}, $g = 2.23$ and $\theta = -1.3$ cm^{-1} for **2**. The efficiency of bipym to transmit electronic effects between iron(II) ions is compared to that of related oxygen-donor potentially bis(chelating) ligands.

The ability of 2,2'-bipyrimidine (bipym) to transmit electronic effects between paramagnetic centres has been a subject of interest over recent years.[1–8] Strong antiferromagnetic coupling [J (singlet–triplet energy gap) ≈ -230 cm^{-1}] is achieved in bipym-bridged copper(II) complexes when the σ in-plane xy exchange pathway (Scheme 1) is operative.[4b,6] The plasticity of the copper(II) co-ordination sphere together with the versatility of bipym as a ligand allows the tuning of the value of J between practically zero and -200 cm^{-1}.[8]

In a recent work, the structural characterization and magnetic study of bipym-bridged nickel(II) dimers ($J \approx -14$ cm^{-1}) revealed that the efficiency of bipym is much decreased when going from copper(II) to nickel(II) complexes.[1] The greater number of unpaired electrons, the occurrence of ferromagnetic terms, the larger M–N(bipym) bond distances and the higher energy of the d orbitals in the case of nickel(II) with respect to copper(II) account for the weaker exchange interaction in the former.

In the present contribution, we report the preparation, structural and magnetic characterization of two bipym-bridged iron(II) complexes of formulae $[Fe_2(H_2O)_8(bipym)][SO_4]_2\cdot 2H_2O$ **1** and $[Fe_2(H_2O)_6(bipym)(SO_4)_2]$ **2**. The exchange interaction between iron(II) ions bridged by bipym and parent bis(chelating) ligands such as oxalate (dianion of oxalic acid, H_2ox) and hydranilate (dianion of 2,5-dihydroxy-1,4-benzoquinone, H_2dhbq) is analysed and discussed in the light of available structural and magnetic data.

Scheme 1

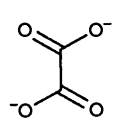

ox

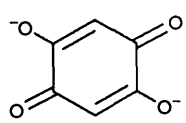

dhbq

Experimental

Materials.—2,2'-Bipyrimidine was purchased from Lancaster Synthesis and used without further purification. Iron(II) sulfate heptahydrate was obtained from Merck and stored under nitrogen. Elemental analyses (C, H, N) were conducted by the Microanalytical Service of the Universidad Autónoma de Madrid (Spain).

† *Supplementary data available:* see Instructions for Authors, *J. Chem. Soc., Dalton Trans.*, 1993, Issue 1, pp. xxiii–xxviii.

Non-SI unit employed: emu = SI × $10^6/4\pi$.

Table 1 Crystallographic data[a] for $[Fe_2(H_2O)_8(bipym)][SO_4]_2 \cdot 2H_2O$ **1** and $[Fe_2(H_2O)_6(bipym)(SO_4)_2]$ **2**

Compound	**1**	**2**
Formula	$C_8H_{26}Fe_2N_4O_{18}S_2$	$C_8H_{18}Fe_2N_4O_{14}S_2$
M	642.1	570.1
Space group	$P2_1/c$	$P2_1/n$
a/Å	8.138(1)	6.275(2)
b/Å	11.661(2)	13.550(4)
c/Å	11.886(2)	10.937(2)
β/°	91.85(1)	96.43(2)
U/Å^3	1127.4(3)	924.1(4)
D_c/g cm^{-3}	1.892	2.049
F(000)	660	580
Crystal size/mm	0.16 × 0.22 × 0.20	0.21 × 0.18 × 0.16
μ(Mo-Kα)/cm^{-1}	15.5	18.7
2θ range/°	3–55	3–54
No. of collected reflections	2920	2305
No of unique reflections	2598	2024
No. of independent reflections[b]	2019	1512
No. of refined parameters, N_p	184	154
$R\{ = [\Sigma(\|\|F_o\| - \|F_c\|\|)/\Sigma\|F_o\|]\}$	0.0274	0.0326
$R'\{ = [\Sigma(\|\|F_o\| - \|F_c\|\|)^2/\Sigma w\|F_o\|^2]^{\frac{1}{2}}\}$	0.0310	0.0336
S[c]	0.963	1.546

[a] Details in common: monoclinic, $Z = 2$, ω–2θ scan method. [b] $I > 3\sigma(I)$. [c] Goodness of fit = $[\Sigma w(\|\|F_o\| - \|F_c\|\|)^2/(N_o\text{-}N_p)]^{\frac{1}{2}}$.

Preparation of $[Fe_2(H_2O)_8(bipym)][SO_4]_2 \cdot 2H_2O$ **1** *and* $[Fe_2(H_2O)_6(bipym)(SO_4)_2]$ **2**.—These compounds were prepared as follows: a solid sample of bipym (0.5 mmol) was added to warm (*ca.* 40 °C) deoxygenated water (40 cm^3) containing iron(II) sulfate (1 mmol) with continuous stirring and under argon. Compound **2** separates as a brown powder from the resulting deep red solution. Well formed polyhedral red and prismatic brown crystals of **1** and **2**, respectively were formed by slow evaporation at room temperature. They were collected by vacuum filtration, washed with ethanol and diethyl ether and stored under calcium chloride. Only crystals of **1** were obtained by recrystallization of the brown powder. Both complexes are stable in air. Precipitation of small amounts of iron(III) hydroxide accompanies the formation of crystals of **1** and **2** when their synthesis is carried out in air. The occurrence of a very asymmetric doublet at 1575s and 1560w cm^{-1} (ring-stretching modes of bipym) in the IR spectra of **1** and **2** are the proof of the bis(chelating) co-ordination mode of this organic ligand as observed in bipym-bridged copper(II) and nickel(II) complexes.[1,4,6-8] In fact, quasi-symmetric doublets at 1564vs and 1555vs cm^{-1} for unco-ordinated bipym[9] and at 1580s(sh) and 1560s(sh) cm^{-1} for chelating bipym[7-8b,10] were reported. Diffuse reflectance spectra of **1** and **2** exhibit a broad maximum at 10 400 cm^{-1} and a stronger absorption at *ca.* 19 000 cm^{-1}. These features are due to unresolved d–d and metal-to-ligand charge-transfer transitions respectively. The aqueous electronic spectrum of these complexes reveals that the dimeric entity is present in solution because of the occurrence of an absorption at 10 400 cm^{-1} (ε *ca.* 7 dm^3 mol^{-1} cm^{-1}). However, some dissociation should occur because of the appearance of two peaks at 20 800 and 27 400 cm^{-1} which are assigned to metal-to-ligand charge-transfer bands of the $[Fe(bipym)_3]^{2+}$ low-spin complex.[11] The extent of this rearrangement must be low because of the reduced values of the molar absorption coefficient of these bands (*ca.* 150 dm^3 mol^{-1} cm^{-1}) with respect to those quoted for the $[Fe(bipym)_3]^{2+}$ species (*ca.* 1000 dm^3 mol^{-1} cm^{-1}) (Found: C, 14.85; H, 4.20; N, 8.65. Calc. for $C_8H_{26}Fe_2N_4O_{18}S_2$ **1**: C, 14.95; H, 4.05; N, 8.70. Found: C, 16.80; H, 3.35; N, 9.75. Calc. for $C_8H_{18}Fe_2N_4O_{14}S_2$ **2**: C, 16.85; H, 3.15; N, 9.80%).

Physical Techniques.—The infrared spectra were taken on a Perkin Elmer 1750 FTIR spectrophotometer as KBr pellets in the 4000–300 cm^{-1} region. The electronic absorption spectra both as a solid and in aqueous solution were recorded on a Perkin Elmer Lambda 9 spectrometer. Variable-temperature magnetic susceptibility measurements were carried out in the range 4.2–300 K with a fully automated AZTEC DSM8 pendulum-type susceptometer equipped with a TBT continuous-flow cryostat and a Brüker BE15 electromagnet, operating at 1.8 T. The apparatus was calibrated with $Hg[Co(NCS)_4]$. Corrections for the diamagnetism of **1** and **2** were estimated from Pascal's constants[12] as -341×10^{-6} and -315×10^{-6} emu mol^{-1}, respectively.

Crystal Structure Determination and Refinement.—Diffraction data for **1** and **2** were collected at 298 K with a Siemens R3m/V automatic four-circle diffractometer using graphite-monochromated Mo-Kα radiation (λ = 0.710 73 Å). Information concerning crystallographic data collection and refinement of the structures is listed in Table 1. The unit-cell parameters were determined from least-squares refinement of the setting angles of 25 reflections in the 2θ range 15–30°. A total of 2920 (**1**) and 2305 (**2**) reflections were collected by the variable-speed ω–2θ scan method in the 2θ ranges 3–55° (**1**) and 3–54° (**2**) with index ranges $0 \leqslant h \leqslant 10$, $0 \leqslant k \leqslant 15$, $-15 \leqslant l \leqslant 15$ (**1**) and $0 \leqslant h \leqslant 8$, $0 \leqslant k \leqslant 17$, $-13 \leqslant l \leqslant 13$ (**2**); 2598 (**1**) and 2024 (**2**) of them were unique, and from these, 2019 (**1**) and 1512 (**2**) were assumed as observed [$I > 3\sigma(I)$] and used for the refinement of the structures. Examination of three standard reflections, monitored after every 100 reflections, showed no sign of crystal deterioration. Lorentz-polarization and ψ-scan absorption corrections[13] were applied to the intensity data. The maximum and minimum transmission factors were 0.694 and 0.611 for **1** and 0.612 and 0.524 for **2**.

The structures of **1** and **2** were solved by standard Patterson methods with the SHELXTL PLUS program[14] and subsequently completed by Fourier recycling. All non-hydrogen atoms were refined anisotropically. The hydrogen atoms of the water molecules were located on a ΔF map and refined with constraints. The hydrogen atoms of bipym were set in calculated positions and refined as riding atoms. A common fixed isotropic thermal parameter was assigned to all hydrogen atoms. The final full-matrix least-squares refinement, minimizing the function $\Sigma w(\|F_o\| - \|F_c\|)^2$ with $w = 1/[\sigma^2(F_o) + q(F_o)^2]$ [q = 0.001 000 (**1**) and 0.000 223 (**2**)] [with $\sigma^2(F_o)$ from counting statistics], converged at R and R' indices of 0.0274 and 0.0310 for **1** and 0.0326 and 0.0336 for **2**. The number of reflections/number of variable parameters was 11.0 and 9.8 for **1** and **2**, respectively. In the final difference map the residual maxima

Table 2 Final atomic coordinates for compound **1** with estimated standard deviations (e.s.d.s) in parentheses

Atom	*X/a*	*Y/b*	*Z/c*
Fe(1)	0.1866(1)	0.1084(1)	0.1885(1)
N(1)	0.2037(2)	0.0606(2)	0.0077(2)
C(1)	0.3276(3)	0.0791(2)	−0.0621(2)
C(2)	0.3183(3)	0.0452(2)	−0.1732(2)
C(3)	0.1783(3)	−0.0104(2)	−0.2104(2)
N(2)	0.0534(2)	−0.0294(2)	−0.1424(2)
C(4)	0.0708(3)	0.0086(2)	−0.0371(2)
O(1)	0.4276(2)	0.1781(2)	0.2163(2)
O(2)	0.1172(3)	0.1421(2)	0.3540(2)
O(3)	0.1135(2)	0.2743(2)	0.1451(2)
O(4)	0.2686(2)	−0.0581(2)	0.2372(2)
S(1)	0.7296(1)	0.2842(1)	−0.0168(1)
O(5)	0.8402(2)	0.2297(2)	−0.0968(2)
O(6)	0.6079(3)	0.3568(2)	−0.0791(2)
O(7)	0.8287(2)	0.3597(2)	0.0586(2)
O(8)	0.6463(2)	0.1969(2)	0.0480(2)
O(9)	0.3260(3)	0.4096(2)	0.0339(2)

Table 3 Final atomic coordinates for compound **2** with e.s.d.s in parentheses

Atom	*X/a*	*Y/b*	*Z/c*
Fe(1)	0.0490(1)	0.0455(1)	0.2659(1)
O(1)	−0.1301(5)	0.1807(2)	0.2506(3)
O(2)	0.2093(5)	−0.0929(2)	0.2877(2)
O(3)	−0.1662(4)	0.0010(2)	0.3834(2)
N(1)	0.1869(4)	0.0755(2)	0.0943(2)
C(1)	0.3621(6)	0.1297(3)	0.0802(3)
C(2)	0.4468(6)	0.1343(3)	−0.0301(3)
C(3)	0.3459(6)	0.0816(3)	−0.1275(3)
N(2)	0.1688(4)	0.0287(2)	−0.1165(3)
C(4)	0.0981(5)	0.0290(2)	−0.0063(3)
S(1)	0.4146(1)	0.1801(1)	0.4455(1)
O(4)	0.3124(4)	0.1010(2)	0.3684(2)
O(5)	0.4055(6)	0.2718(2)	0.3799(3)
O(6)	0.6391(4)	0.1523(2)	0.4796(2)
O(7)	0.3061(5)	0.1873(2)	0.5571(3)

and minima were 0.33 and −0.36 e Å^{-3} for **1** and 0.57 and −0.40 e Å^{-3} for **2**. The largest and mean Δ/σ are 0.207 and 0.014 for **1** and 0.014 and 0.003 for **2**. Solutions and refinements were performed with the SHELXTL PLUS system.[14] The final geometrical calculations were carried out with the PARST[15] program. The graphical manipulations were performed using the XP utility of the SHELXTL PLUS system. The final atomic coordinates for non-hydrogen atoms and selected bond lengths and angles for compounds **1** and **2** are given in Tables 2–5.

Additional material available from the Cambridge Crystallographic Data Centre comprises H-atom coordinates, thermal parameters and remaining bond lengths and angles.

Results and Discussion

Description of the Structures of Compounds **1** *and* **2**.—The structure of **1** is made up of $[Fe_2(H_2O)_8(bipym)]^{4+}$ dinuclear cations, unco-ordinated sulfate anions and crystallization water molecules, whereas that of **2** consists of neutral $[Fe_2(H_2O)_6(bipym)(SO_4)_2]$ dinuclear units. Compound **1** is isostructural with the parent $[Ni_2(H_2O)_8(bipym)][SO_4]_2\cdot 2H_2O$.[1] In all these complexes, a crystallographically imposed inversion centre is located halfway between the halves of the bipym molecule. The molecular geometry along with the atom labelling scheme for the dinuclear entities of **1** and **2** are depicted in Figs. 1 and 2(*a*), respectively. The sulfate anions and the water molecules contribute to the packing by forming an extensive network of hydrogen bonds (Tables 4 and 5). As shown in Fig. 2(*b*), aqua and sulfato ligands of two dinuclear units of **2** are

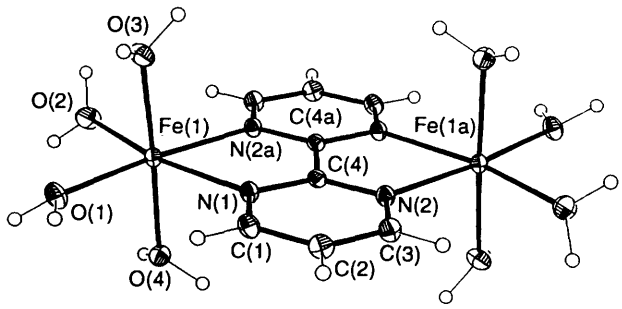

Fig. 1 An ORTEP drawing of the cationic unit $[Fe_2(H_2O)_8(bipym)]^{4+}$ of **1** showing the atom labelling. Thermal ellipsoids are drawn at the 30% probability level

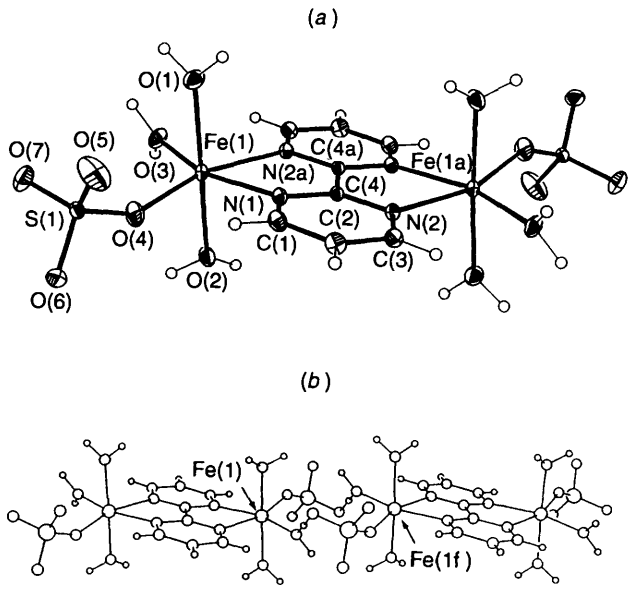

Fig. 2 (*a*) An ORTEP drawing of **2** showing the atom labelling; thermal ellipsoids are drawn at the 30% probability level. (*b*) A view of the polymerisation of **2** through hydrogen-bonding interactions

linked through hydrogen bonding to yield a one-dimensional arrangement, the resulting intermolecular Fe(1)···Fe(1f) separation being 5.370(1) Å.

The iron atoms in both compounds are six-co-ordinate, FeN_2O_4: two nitrogen atoms from bipym and four oxygen atoms either from four water molecules in **1** or from one unidentate sulfate group and three water molecules in **2** build a distorted octahedron around the metal ion. The Fe–N(bipym) bond lengths lie in the range 2.191(3)–2.247(3) Å and are close to those reported for the dinuclear complex $[\{Fe(bipym)(NCS)_2\}_2(bipym)]$[5] where both chelating and bis(chelating) bipym are present. However, they are significantly longer than the Fe–O bond lengths (average values 2.11 and 2.09 Å for **1** and **2**, respectively). The presence of co-ordinated sulfate in **2** causes a greater distortion of the metal environment in this compound. So, the shorter and longer Fe–O bonds are 2.085(2) and 2.138(2) Å in **1** whereas they are 2.035(3) and 2.147(3) Å in **2**. Furthermore, the O(1)–Fe(1)–O(2) angle in **1** [93.3(1)°] is much smaller than the related O(3)–Fe(1)–O(4) one in **2** [108.3(1)°]. The best equatorial plane is defined by the N(1), N(2a), O(1) and O(2) atoms [largest deviation from the mean plane is 0.026(2) Å for O(2)] in **1** and by the N(1), N(2a), O(3) and O(4) atoms [largest deviation is 0.111(3) Å for N(1)] in **2**. The iron atom is 0.010(1) (**1**) and 0.060(1) Å (**2**) out of these planes. A large deviation from the idealized orthogonal geometry is found at the metal atom in the five-membered Fe(1)N(1)C(4)-C(4a)N(2a) chelate ring [74.9(1) and 74.1(1)° for N(1)–Fe(1)–N(2a) in **1** and **2**, respectively] as expected due to the

Table 4 Selected interatomic distances (Å) and bond angles (°) for **1** with e.s.d.s. in parentheses[a]

Iron environment

Fe(1)–O(1)	2.138(2)	Fe(1)–O(4)	2.127(2)
Fe(1)–O(2)	2.101(2)	Fe(1)–N(1)	2.229(2)
Fe(1)–O(3)	2.085(2)	Fe(1)–N(2a)	2.213(2)
N(1)–Fe(1)–N(2a)	74.9(1)	N(2a)–Fe(1)–O(4)	87.4(1)
N(1)–Fe(1)–O(1)	99.1(1)	O(2)–Fe(1)–O(1)	93.3(1)
N(1)–Fe(1)–O(2)	167.6(1)	O(2)–Fe(1)–O(3)	88.5(1)
N(1)–Fe(1)–O(3)	91.1(1)	O(2)–Fe(1)–O(4)	90.4(1)
N(1)–Fe(1)–O(4)	90.3(1)	O(1)–Fe(1)–O(3)	86.5(1)
N(2a)–Fe(1)–O(2)	92.8(1)	O(1)–Fe(1)–O(4)	91.5(1)
N(2a)–Fe(1)–O(1)	173.9(1)	O(3)–Fe(1)–O(4)	177.7(1)
N(2a)–Fe(1)–O(3)	94.7(1)		

Hydrogen bonds[b]

A	D	H	A···D	A···H–D
O(8)	O(1)	H(1w)	2.73(1)	172(3)
O(9)	O(3)	H(6w)	2.72(1)	176(3)
O(6)	O(9)	H(10w)	2.77(1)	166(2)
O(6b)	O(1)	H(2w)	2.83(1)	174(3)
O(9b)	O(2)	H(4w)	2.75(1)	163(2)
O(5c)	O(2)	H(3w)	2.78(1)	170(2)
O(7d)	O(4)	H(8w)	2.75(1)	178(2)
O(7e)	O(3)	H(6w)	7.70(1)	169(3)
O(5f)	O(4)	H(7w)	2.73(1)	160(3)
O(6g)	O(9)	H(10w)	2.82(1)	164(2)

[a] Symmetry code: (a) $-x, -y, -z$; (b) $x, \frac{1}{2}-y, \frac{1}{2}+z$; (c) $x-1, \frac{1}{2}-y, \frac{1}{2}+z$; (d) $1-x, y-\frac{1}{2}, \frac{1}{2}-z$; (e) $x-1, y, z$; (f) $1-x, -y, -z$; (g) $1-x, 1-y, -z$. [b] A = Acceptor, D = donor.

Table 5 Selected interatomic distances (Å) and bond angles (°) for **2** with e.s.d.s. in parentheses[a]

Iron environment

Fe(1)–O(1)	2.147(3)	Fe(1)–O(4)	2.035(3)
Fe(1)–O(2)	2.128(3)	Fe(1)–N(1)	2.191(3)
Fe(1)–O(3)	2.057(3)	Fe(1)–N(2a)	2.247(3)
N(1)–Fe(1)–N(2a)	74.1(1)	N(2a)–Fe(1)–O(2)	85.9(1)
N(1)–Fe(1)–O(4)	91.7(1)	O(3)–Fe(1)–O(4)	108.3(1)
N(1)–Fe(1)–O(3)	160.0(1)	O(3)–Fe(1)–O(1)	85.6(1)
N(1)–Fe(1)–O(1)	91.6(1)	O(3)–Fe(1)–O(2)	90.4(1)
N(1)–Fe(1)–O(2)	91.9(1)	O(4)–Fe(1)–O(1)	96.5(1)
N(2a)–Fe(1)–O(3)	86.3(1)	O(4)–Fe(1)–O(2)	85.4(1)
N(2a)–Fe(1)–O(4)	163.1(1)	O(1)–Fe(1)–O(2)	176.0(1)
N(2a)–Fe(1)–O(1)	93.1(1)		

Hydrogen bonds[b]

A	D	H	A···D	A···H–D
O(6b)	O(3)	H(6w)	2.66(1)	158(3)
O(7c)	O(1)	H(2w)	2.76(1)	177(3)
O(5d)	O(2)	H(3w)	2.63(1)	158(2)
O(6e)	O(2)	H(4w)	2.74(1)	174(3)
O(7f)	O(3)	H(5w)	2.80(1)	169(2)

[a] Symmetry code: (a) $-x, -y, -z$; (b) $x-1, y, z$; (c) $x-\frac{1}{2}, \frac{1}{2}-y, z-\frac{1}{2}$; (d) $\frac{1}{2}-x, y-\frac{1}{2}, \frac{1}{2}-z$; (e) $1-x, -y, 1-z$; (f) $-x, -y, 1-z$. [b] A = Acceptor, D = donor.

short bite distance of the free bipym (2.63 Å).[16] The value of this angle at the nickel atom in the related bipym-bridged nickel(II) complex is 78.5(1)°. Such a decrease in the angle subtended by bipym at the metal atom when passing from nickel(II) to iron(II) is related to the lengthening of the metal–nitrogen(bipym) bonds in the latter.

The pyrimidyl rings of bipym are planar as expected with deviations from the mean planes not greater than 0.015(2) Å in **1** and 0.010(4) Å in **2**. The bipym ligand as a whole is also planar in both complexes. The carbon–carbon and carbon–nitrogen intra-ring bond distances agree with those observed in other bipym-bridged metal complexes.[1,3–8] The carbon–carbon inter-ring bond length [1.488(4) and 1.480(6) Å in **1** and **2**, respectively] is close but somewhat shorter than the classical value of 1.54 Å for the single carbon–carbon bond distance. The iron atom is 0.043(1) (**1**) and 0.249(1) Å (**2**) out of the bipym plane. The dihedral angle between the bipym and the equatorial planes N(1)N(2a)O(1)O(2) of **1** and N(1)N(2a)O(3)O(4) of **2** is 2.4(1) and 10.9(1)°, respectively.

The metal–metal separation through bipym, Fe(1)···Fe(1a), is 5.836(1) Å in **1**, 5.909(1) Å in **2**, and 5.522(6) Å in $[\{Fe(bipym)(NCS)_2\}_2(bipym)]$,[5] the trend followed being monitored by the Fe–N(bipym) distances. The shortest intermolecular metal–metal distance is 6.696(1) Å [Fe(1)···Fe(1h) and Fe(1)···Fe(1i); symmetry codes: (h) $-x, y-\frac{1}{2}, \frac{1}{2}-z$ and (i) $-x, \frac{1}{2}-y, \frac{1}{2}-z$] in **1** and 5.370(1) Å [Fe(1)···Fe(1f)] in **2**.

The sulfate ions have their expected tetrahedral geometry [average values of the sulfur–oxygen bond distance are 1.473 (**1**) and 1.458 Å (**2**) and the average intra-ion bond angle is 109.5°]. In both complexes the molecules are held together by hydrogen bonds involving water molecules and sulfate anions. In particular, in **1** a crystallization water molecule binds to two co-ordinated water molecules belonging to two different Fe(bipym)Fe units; the resulting metal–metal distance is 6.743(1) Å. In **2**, the pair of hydrogen bonds between O(3) and O(7f) is particularly important as it contributes to the formation of a 12-membered ring involving two sulfate groups, two co-ordinated water molecules and two iron(II) ions [Fig. 2(*b*)]. The distance between these metal ions [5.370(1) Å for Fe(1)···Fe(1f)] is smaller than the intramolecular metal–metal separation.

Magnetic Properties.—The magnetic properties of **1** and **2** in the form of both χ_M (molar magnetic susceptibility) and $\chi_M T$ *versus* T plots are depicted in Figs. 3 and 4. The curves of susceptibility show rounded maxima at 15.1 and 15.7 K for **1** and **2**, respectively whereas those of $\chi_M T$ exhibit a continuous decrease upon cooling down, with $\chi_M T = 7.46$ (**1**) and 7.15 $cm^3 mol^{-1} K$ (**2**) at 290 K and an extrapolated value that vanishes when T approaches to zero. Such a behaviour is characteristic of an intramolecular antiferromagnetic interaction between two high-spin iron(II) ions, with a molecular spin singlet ground state. We have attempted to reproduce theoretically the experimental susceptibility of **1** and **2** by use of the Heisenberg–Dirac–Van-Vleck $S_A = S_B = 2$ spin-coupled dimer model with the spin Hamiltonian $\hat{H} = -J\hat{S}_A \cdot \hat{S}_B$. The parameters J, g and θ (intermolecular interactions) were determined by least-squares fit minimizing $R = \Sigma[(\chi_M)_{obs} - (\chi_M)_{calc}]^2/\Sigma[(\chi_M)_{obs}]^2$. The values obtained were $J = -3.4\ cm^{-1}$, $g = 2.28$, $\theta = -0.7\ cm^{-1}$ and $R = 2.7 \times 10^{-3}$ for **1** and $J = -3.1\ cm^{-1}$, $g = 2.23$, $\theta = -1.3\ cm^{-1}$ and $R = 8 \times 10^{-4}$ for **2**. An inspection of the computed curves (Figs. 3 and 4) shows that the experimental data are reproduced by the spin-only formula, although a satisfactory match to the experimental data is not achieved. Most likely, the orbital contribution is small due to the low symmetry (roughly C_{2v} for **1** and **2**) but not totally negligible. In this regard, the lower distortion of **1** with respect to **2** because of the occurrence of co-ordinated sulfate in **2**, accounts for the better fit found in the latter compound. Dealing with the intermolecular magnetic interaction, the shorter intermolecular metal–metal separation in **2** [hydrogen bonding between sulfato and aqua ligands, Fig. 2(*b*)], leads to a greater θ value in this compound. The real $|J|$ values should be slightly larger than the computed ones as inferred from the relative positions of the computed and experimental maxima. Finally, the fit was not significantly improved and the J values remained practically unchanged when the local anisotropy of the iron(II) ion was introduced in the calculation.

The J values of compounds **1** and **2** are practically identical as expected in the light of their closely related crystal structures. The ligand bipym acts as a bridge between the metal atoms and

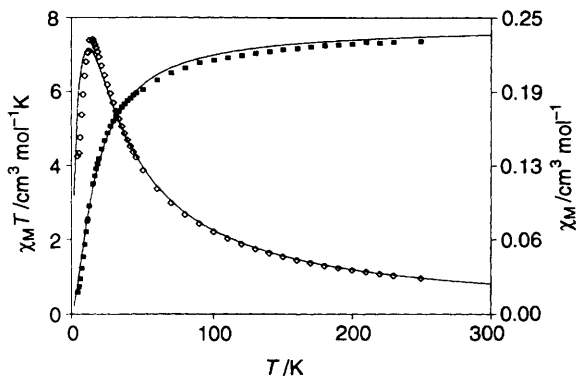

Fig. 3 Thermal dependence of the molar magnetic susceptibility χ_M (◇) and $\chi_M T$ (■) for **1**. The solid line corresponds to the best theoretical fit (see text)

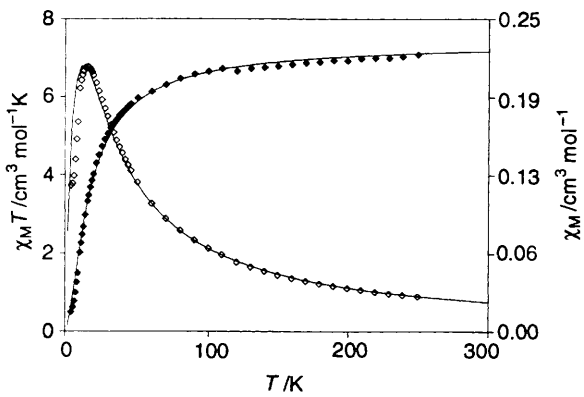

Fig. 4 Thermal dependence of the molar magnetic susceptibility χ_M (◇) and $\chi_M T$ (◆) for **2**. The solid line corresponds to the best theoretical fit (see text)

the resulting intramolecular iron–iron separation is nearly identical. As shown previously,[4b,17] this kind of bis(chelating) ligand (Scheme 1) leads to an antiferromagnetic interaction between metal centres if a magnetic orbital of *xy* symmetry is available on each interacting metal ion. Obviously, this exchange pathway is operative with iron(II). Only the crystal structure of a bipym-bridged iron(II) complex of formula $[\{Fe(bipym)(NCS)_2\}_2(bipym)]$ was known prior to the present work and a value of $J = -4.1$ cm^{-1} was found.[5] The fact that the antiferromagnetic coupling in **1** and **2** is somewhat weaker can be easily understood taking into account that the intramolecular metal–metal separation is about 0.3 Å shorter for the latter compound [5.522(6) Å].

Concerning the exchange coupling in polynuclear iron(II) complexes, a comparison of the relative ability of potentially bis(chelating) bipym, oxalate and hydranilate systems to transmit electronic effects is in order. Concerning the oxalato-bridged iron(II) complexes, only the structure of $[\{Fe(ox)(H_2O)_2\}_n]$[18] was reported. It consists of one-dimensional iron(II) chains in which oxalate acts as a bis(bidentate) bridging ligand. Although no structure for dhbq-bridged iron(II) complexes has been published, structural information concerning other metal complexes of dihydroxybenzoquinones,[19–23] reasonably support the bis(chelating) co-ordination mode for dhbq in the polymer of formula $Fe(dhbq)(H_2O)_2$.[24] As far as the complexes $[\{Fe(ox)(H_2O)_2\}_n]$ and $Fe(dhbq)(H_2O)_2$ are concerned, the metal ions are antiferromagnetically coupled with *J* values of −8.8 and −2.8 cm^{-1}, respectively.[24,25] The trend exhibited by the *J* values in this family of iron(II) complexes is $|J|_{ox} > |J|_{bipym} > |J|_{dhbq}$. The larger coupling would correspond to bipym because the less electronegative the atoms of the bridge are, the higher the delocalization of the spin density on them, and consequently, the greater the antiferromagnetic coupling[26,27] everything being equal. However, the greater stabilization by resonance of the symmetry-adapted highest occupied molecular orbitals (HOMOs) of bipym that overlap with the in-phase and out-of-phase combinations of the d_{xy} magnetic orbitals of iron(II) causes a smaller overlapping in this case with respect to that of oxalate, and accounts for the weaker coupling. Another factor to be taken into account is the metal–metal separation through the bridges.[28,29] This factor is not relevant for bipym and oxalate because such a separation varies between 5.6 and 5.9 Å. However, an iron–iron separation through dhbq larger than 7.6 Å can be easily calculated and such a large separation is most likely at the origin of the lower efficiency of dhbq with respect to ox.

Acknowledgements

Financial support from the Dirección General de Investigación Científica y Técnica (DGICYT) (Spain) through Project PB91-0807-C02-01 and from the Italian Ministero dell'Università e della Ricerca Scientifica e Tecnologica are gratefully acknowledged. Thanks are also due to the Servicio de Espectroscopía de la Universitat de València for instrumental facilities.

References

1 G. De Munno, M. Julve, F. Lloret and A. Derory, *J. Chem. Soc., Dalton Trans.*, 1993, 1179.
2 R. H. Petty, B. R. Welch, L. J. Wilson, L. A. Bottomley and K. M. Kadish, *J. Am. Chem. Soc.*, 1980, **102**, 611; G. A. Brewer and E. Sinn, *Inorg. Chem.*, 1984, **23**, 2532.
3 G. Brewer and E. Sinn, *Inorg. Chem.*, 1985, **24**, 4580.
4 (*a*) G. De Munno and G. Bruno, *Acta Crystallogr., Sect. C*, 1984, **40**, 2030; (*b*) M. Julve, G. De Munno, G. Bruno and M. Verdaguer, *Inorg. Chem.*, 1988, **27**, 3160.
5 J. A. Real, J. Zarembowitch, O. Kahn and X. Solans, *Inorg. Chem.*, 1987, **26**, 2939.
6 M. Julve, M. Verdaguer, G. De Munno, J. A. Real and G. Bruno, *Inorg. Chem.*, 1993, **32**, 795.
7 G. De Munno, M. Julve, F. Nicolò, F. Lloret, J. Faus, R. Ruiz and E. Sinn, *Angew. Chem., Int. Ed. Engl.*, 1993, **32**, 613.
8 (*a*) G. De Munno, M. Julve, M. Verdaguer and G. Bruno, *Inorg. Chem.*, in the press; (*b*) L. W. Morgan, K. V. Goodwin, W. T. Pennington and J. D. Petersen, *Inorg. Chem.*, 1992, **31**, 1103.
9 N. Neto, G. Sabrana and N. Muniz-Miranda, *Spectrochim. Acta, Part A*, 1990, **46**, 705.
10 G. De Munno, G. Bruno, M. Julve and M. Romeo, *Acta Crystallogr., Sect. C*, 1990, **46**, 1828; L. W. Morgan, W. T. Pennington, J. D. Petersen and R. R. Ruminski, *Acta Crystallogr., Sect. C*, 1992, **48**, 163; I. Castro, M. Julve, G. De Munno, G. Bruno, J. A. Real, F. Lloret and J. Faus, *J. Chem. Soc., Dalton Trans.*, 1992, 1739.
11 R. R. Ruminski and J. D. Petersen, *Inorg. Chim. Acta*, 1993, **97**, 129.
12 A. Earnshaw, *Introduction to Magnetochemistry*, Academic Press, London and New York, 1968.
13 A. C. T. North, D. C. Phillips and F. S. Mathews, *Acta Crystallogr., Sect. A*, 1968, **24**, 351.
14 SHELX PLUS, Version 3.4, Siemens Analytical X-ray Instruments Inc., Madison, WI, 1989.
15 M. Nardelli, *Comput. Chem.*, 1983, **7**, 95.
16 L. Fernholt, C. Rømming and S. Samdal, *Acta Chem. Scand., Ser. A*, 1981, **35**, 707.
17 O. Kahn, *Angew. Chem., Int. Ed. Engl.*, 1985, **24**, 834 and refs. therein.
18 S. Cavid, *Bull. Soc. Fr. Mineral Cristallogr.*, 1959, **82**, 50.
19 C. G. Pierpont, L. C. Francesconi and D. N. Hendrickson, *Inorg. Chem.*, 1977, **16**, 2367.
20 M. Verdaguer, A. Michalowicz, J. J. Girerd, N. Alberding and O. Kahn, *Inorg. Chem.*, 1980, **19**, 3271; F. Tinti, M. Verdaguer, O. Kahn and J. M. Savariault, *Inorg. Chem.*, 1987, **26**, 2380.
21 S. Liu, S. N. Shaikn and J. Zubieta, *J. Chem. Soc., Chem. Commun.*, 1988, 1017.
22 J. V. Folgado, R. Ibáñez, E. Coronado, D. Beltrán, J. M. Savariault and J. Galy, *Inorg. Chem.*, 1988, **27**, 19.
23 S. Cueto, H. P. Straumann, P. Rys, W. Petter, V. Gramlich and F. S. Rys, *Acta Crystallogr., Sect. C*, 1992, **48**, 458.
24 J. T. Wrobleski and D. B. Brown, *Inorg. Chem.*, 1979, **18**, 498.
25 J. T. Wrobleski and D. B. Brown, *Inorg. Chem.*, 1979, **18**, 2738.

26 M. Verdaguer, O. Kahn, M. Julve and A. Gleizes, *Nouv. J. Chim.*, 1985, **9**, 325.
27 S. Alvarez, M. Julve and M. Verdaguer, *Inorg. Chem.*, 1990, **29**, 4500.
28 R. E. Coffman and G. R. Buettner, *J. Phys. Chem.*, 1979, **83**, 2387.
29 D. N. Hendrickson, in *Magneto-Structural Correlations in Exchange Coupled Systems*, eds. R. D. Willett, D. Gatteschi and O. Kahn, NATO-ASI Series, Reidel, Dordrecht, 1985, p. 523.

Received 22*nd January* 1993; *Paper* 3/00406F